



NUMERICAL APPROACH TO ASSESS SEQUENTIAL EARTHQUAKE AND TSUNAMI DAMAGE ON A PILE SUPPORTED QUAY

C. Reis⁽¹⁾, M. Lopes⁽²⁾, S. Clain⁽³⁾, M.A. Baptista⁽⁴⁾

⁽¹⁾ PhD student, Civil Engineering Research Innovation for Sustainability, Instituto Superior Técnico, Universidade de Lisboa, claudia.reis@tecnico.ulisboa.pt

⁽²⁾ Professor, Civil Engineering Research Innovation for Sustainability, Instituto Superior Técnico, Universidade de Lisboa, mariolopes@tecnico.ulisboa.pt

⁽³⁾ Professor, Departamento de Matemática e Aplicações, Universidade do Minho, clain@math.uminho.pt

⁽⁴⁾ Professor, Departamento de Engenharia Civil, Instituto Superior de Engenharia de Lisboa, mavbaptista@gmail.com

Abstract

Ports are strategic socioeconomical structures that may be affected by catastrophic natural hazards, like earthquakes and their subsequent tsunamis. To mitigate the effects of cascading earthquake and tsunami hazards on ports, it is necessary to design performance-efficient portuary structures against the succession of earthquake and tsunami actions.

In this paper, we present a new numerical model to determine the structural response of a pile-supported quay of a deep-water European port, Sines (Portugal), currently in phase of expansion, to the succession of seismic and tsunami actions. The model uses a multi-target-hazard assessment considering multiple scenarios to account for the source uncertainty. The structural response is characterized by a double dynamic non-linear analysis method, considering the time-histories of the strong motion acceleration and the hydrodynamic tsunami force. The structural behavior of the pile-supported quay is inferred through capacity curves accounting for the influence of the cascading nature of the actions.

We briefly discuss recommending design measures to mitigate the effects of a successive earthquake-tsunami impact on portuary structures. Accordingly, design solutions are suggested, for new or on rehabilitation phases, allowing to minimize the damages of the pile-supported quays.

Keywords: Cascading earthquake and tsunami; Earthquake and tsunami damage; Port structures; Pile-supported quay

1. Introduction

The human casualties and economic losses due to tsunami impact have significantly increased over the two last decades [1]. The world population doubled in the last forty years and the United Nations, UN, refers about 50% of the population living within 100 km of the coast and 10% living in coastal areas that are less than 10m above sea level. In 2015, the UN Office for Disaster Risk Reduction developed a 15-year framework to reduce the risk, the Sendai Framework [2]. However, 90% of the funding is to reconstruction and damage response and only 10% to prevention actions.

Important and strategic structures, such as ports, require a perspective of resilience in a preventive stage. Besides the fundamental role in economic and social aspects, ports are also part of the post-disasters aid for the community, highlighting the importance of preventive measures to mitigate the effect of near-field tsunamis with tectonic origin in portuary regions. By adopting structural design criteria, attending for successive strong motions and tsunami, is possible to guarantee the serviceability of ports after these extreme natural phenomena. However, only recently two countries included the tsunami action in their design codes, United States [3] and Japan [4], nevertheless both neglecting the cascading aspect of the succession of actions. Even the empirical fragility functions developed after recent important events neglect the influence of the earthquake prior to the tsunami, assuming the questionable premise that earthquake damage is minimal compared to tsunami hazard [5]. The behavior of a structure previously submitted to an earthquake with magnitude greater than M7.5, is potentially constrained for the income tsunami.

Despite the paucity of regulation, an incipient investigation on the cascading effects is being undertake concerning coastal protection structures [6], quay walls of wharves [7], buildings [8] and bridges [9]. However,



the innovative topic remains a challenge due to the novelty of the investigation and the infrequent nature of such events. Lacks recorded information for generation of synthetic data and observation data to characterize structural behavior. In addition, survey teams struggle to separate earthquake- from tsunami-induced damage [10]. The few data available is used for the validation of experimental and numeric approaches. In opposition to the more costly and time-consuming experimental approaches, the numerical tools provide valuable contributions for the investigation. The counterpart is the complexity of the numerical models required to solve the sophisticated governing equations, leading to high computational costs.

In this paper, a new numeric methodology being developed in the framework of the doctoral thesis of the first author, is tested to investigate the cascading effects of strong motion and tsunami in a pile-supported quay. These structures are relatively new in comparison to gravity or sheet-pile solutions. Therefore, besides the common difficulties mentioned, and despite the exhaustive survey of ports damage after the 2011, Japan earthquake and tsunami, their structural behavior remains poorly documented [11]. The case-study regards the terminal container, Terminal XXI, implemented in the Sines port, in Portugal. The Portuguese tectonic context is characterized by moderate to large onshore and offshore activity, with tsunamigenic potential [12]. The problem is tackled from the tsunamigenic deterministic hazard to the resistance of the structural elements, aiming to optimize the structural design by:

- target-defining the cascading strong ground motion and tsunami actions.
Typically, the worldwide design standards recommend uniform-hazard maps for the definition of the seismic acceleration (peak value or time-history). The American design code [3] already considers risk-targeted seismic and tsunami design maps [13]. In some regions of EUA, the use of seismic target-hazard maps have decreased the seismic forces for the design process by 30% compared to corresponding uniform-hazard maps [14]. In Europe, the design code Eurocode [15], considers uniform probabilistic seismic hazard maps and the tsunami action is not addressed yet. The inclusion of seismic target-hazard in future versions of Eurocode is being discussed [16] [17], as well as the tsunami as an acting load on coastal structures [18]. In this paper, is considered the seismic uncertainty associated to a 1755-type event, most probably triggered at the Southwest Iberia Margin, SWIM [19] [20] [21]. By identifying, computing [22] [23] and comparing the results of the different faults' scenarios, we assessed the worst case scenario and determine the peak of the inundation depth and flow velocity to characterize the tsunami action, and the corresponding peak of the strong ground motion acceleration to characterize the earthquake action;
- performing a successive structural analysis.
Previous studies show that, function of the simplicity of geometry and loading conditions, two-dimensions, 2D, models provide globally similar results to three-dimensions, 3D, models [24]. Due to its geometric regularity, the pile-supported quay is modeled in 2D. The reinforced-concrete, RC, frame is discretized by non-linear materials with progressively stiffness degradation. The time-histories of the earthquake acceleration and the hydrodynamic tsunami force are applied as signals to excite the structure. To assess the structural behavior, is performed a double non-linear dynamic analysis to the structure, considering the succession of strong ground motion and tsunami actions. The structural response, in terms of forces and deformations, is compared to the structural capacity curve. Being the current work an investigation in progress, we briefly introduce future works and discuss preventive design measures to mitigate the earthquake-tsunami effects in general pile-supported quays.

To the best of the authors knowledge, beside the novelty of coastal structures subjected to cascading earthquake and tsunami actions, the paper is also innovative due to 1) the object of study – relatively new solution of pile-supported wharves whose structural dynamic behavior is poorly documented; and 2) the domain of the problem – tackled from the geophysical assessment of the extreme natural phenomena to the structural analysis of the elements, allowing to consider the seismic uncertainty.



2. Methodology

To assess and discuss the structural behavior of a pile-supported quay under the cascading seismic and tsunami actions, we follow three complementary stages.

The first stage regards the target-hazard assessment of the region and the determination of the respective time-histories of the seismic and tsunami actions possible to be exerted against the structure. We establish the possible tsunami scenarios by identifying and characterizing local and regional tsunamigenic sources, in terms of epicentral location and focal mechanism. We adopt the half-space theory of Okada [25], implemented in Mirone suite [26], to calculate the vertical deformation that triggered the tsunami. The computation of the propagation and inundation phases is performed by our home-developed solver of the non-linear Shallow-Water equations, NLSWE, based on the Finite Volume Method, FVM. The presentation and validation of our numerical tool, Kotkot, is detailed in Clain et al., 2016 [22] and Reis et al., 2018 [23]. The system of equations, with varying bathymetry, follows Eq. (1):

$$\begin{cases} \partial_t h + \partial_x(hu) + \partial_y(hv) = 0, \\ \partial_t(hu) + \partial_x(hu^2 + \frac{g}{2}h^2) + \partial_y(huv) = -gh\partial_x b, \\ \partial_t(hv) + \partial_x(huv) + \partial_y(hv^2 + \frac{g}{2}h^2) = -gh\partial_y b \end{cases} \quad (1)$$

where, $\partial_t h$ is the water height, ∂u and ∂v velocity components and b the topo-bathymetry.

We select the worst-case scenario by comparing the resultant inundation depths and flow velocity. We follow the analytic formulation recommended by ASCE [3] to obtain the time-history of the tsunami hydrodynamic action, in the horizontal and vertical directions, in Eqs. (2) and (3), respectively:

$$F_{hd_h} = \frac{1}{2} \rho I_{tsu} C_d C_{cx} B hu^2 \quad (2)$$

where, the geometry of the structure is represented in the equation by B as the structure width, C_d drag coefficient (ratio B/h), C_{cx} the closure coefficient and I_{tsu} is the importance factor function of the structure's importance. The fluid is represented by ρ water density and hu^2 momentum flux combining water depth and velocity.

$$F_{hd_v} = \frac{1}{2} \rho C_u A_f u^2 \quad (3)$$

where, C_u is the uplift coefficient and A_f the cross-sectional area of the quay deck.

For the sake of consistency, and to avoid a too conservative structural design, we select the seismic source that generated the tsunami worst-case scenario to compute the time-histories of the ground strong motion accelerations. The simulation is performed by an adapted version of a well-known software used to simulate stochastic accelerations from finite faults, FINSIM [27]. The adaptation, by Laboratório Nacional de Engenharia Civil, LNEC-FINSIM [28], includes a non-stationary stochastic finite fault simulation method, based on Boore's theory [29], Eq. (4):

$$A(f, M_0, R) = (2\pi f)^2 \cdot C \cdot S \cdot G \cdot A_n \cdot A_{tc} \quad (4)$$

The amplitude spectrum is function of f frequency of the seismic wave, M_0 seismic moment and R distance to the source. The equation considers the earthquake source, using the displacement source spectrum, S , affected by a scaling factor, C ; the propagation of the wave affected by a geometric attenuation factor, G ; and, local attenuation and amplification effects, $A_n \cdot A_{tc}$. At least, from the seismic and tsunami synthetic time-histories, we assess the respective peak ground acceleration and peak hydrodynamic effect.

The second stage regards the computation of the structural response. We use an open-source software, Open System for Earthquake Engineering Simulations, OpenSees [30], a framework based on Finite Element Method, FEM, to compute the response of our structural and geotechnical systems, with two dimensions and three degrees of freedom, two translational and one rotational. The quay deck, the column and the piles are



modeled as RC non-linear distributed plasticity column and beams, allowing the formation of plastic hinges along the length of the elements, particularly near the members edges, where plasticity is typically concentrated. Nonlinearities are assigned by fiber sections definition, considering confined and unconfined concrete and reinforcement steel bars, modeled by *Force-based Beam-Column* elements with *Force-Deformation* fiber sections. The uniaxial stress-strain of concrete fibers are modeled to account axial, flexure and shear stresses, based on the *Concrete04* material, characterized by hysteretic unloading/reloading branches including compression and linear tension softening to define the confined and unconfined concrete stress-strain behavior. The steel fibers are modeled with a bilinear stress-strain relation with isotropic kinematic hardening in tension and compression, *Steel02* material. The materials models allow material stiffness degradation.

The permanent loading accounts with the dead weight of the RC elements in the area of influence of each frame. For the live loading, we consider a uniformly distributed load in along the beams length and neglect, at this incipient stage of the work, the ships mooring, and the moving loads associated with cranes and reach stackers. Rayleigh damping is assumed 5% proportion to mass and stiffness, characterized after a modal analysis of the structure. The earthquake action is represented by ten acceleration signals. The hydrodynamic action is applied in the horizontal and vertical directions.

The European design code [15] recommends the seismic loading combination, as in Eq. (5):

$$S_E = DL + 0.5 LL + 1.5 E \quad (5)$$

where, DL and LL are gravity loads acting the structure, respectively, dead and live loads. E is the earthquake load.

The American design code [3] recommends the tsunami loading combinations, as in Eq. (6):

$$\begin{cases} S_{T1} = 0.9 DL + F_T + 1.2 H \\ S_{T2} = 1.2 DL + F_T + 0.5 LL + 0.2 S + 1.2 H \end{cases} \quad (6)$$

where, DL and LL are dead and live loads. F_T is the tsunami load, S is the snow load and H the load due to lateral earth or ground water pressure.

The structural analysis is performed by a non-linear dynamic approach. The first interval, modal and linear static interval, characterize the structural elastic behavior due to gravity loads. The second, non-linear transient dynamic analysis, characterizes the behavior due to the ground accelerations. A subsequent assessment of the elastic/plastic regime of the structure is performed prior to the income tsunami. Finally, the third, is also a non-linear dynamic analysis, to assess the effects of the vertical hydrodynamic force and the combination of ground motion and lateral hydrodynamic force. For the verification of the tsunami vertical effects, we compare uplifting and gravity forces. The analyses provide data on the applied loading patterns and the structural inelastic response, identifying the probable development of plastic hinges. The outputs are validated with previous studies of the structure and compared to the design damage limitation criteria.

The third stage regards a brief discussion on future works, regarding the level of complexity of the determination of both the seismic actions, strong ground motions and tsunami (deterministic vs. probabilistic), the structural model (2D vs. 3D; level of discretization of the structure-soil interaction system, discrete vs. continuum). We also tackle mitigation measures to the successive earthquake and tsunami effects on coastal structures, namely, the presence vs. absence of coastal defense structures, and/or, structural solutions.

3. Case-Study

Our case-study regards the pile-supported quay, Terminal XXI, of the Sines port, in southwest coast of Portugal. The Portuguese region has onshore moderate to large tectonic activity, and large to very large offshore earthquakes that have generated tsunamis in the paste [12]. The most studied event is the probable magnitude 8.5 ± 0.3 earthquake and tsunami event, occurred in the 1st of November 1755. Nevertheless, the location of the source and the rupture mechanism remain a matter of debate, pointing the faults of the SWIM zone, depicted in Fig. 1a, as the most probable to have triggered the event [19] [20].

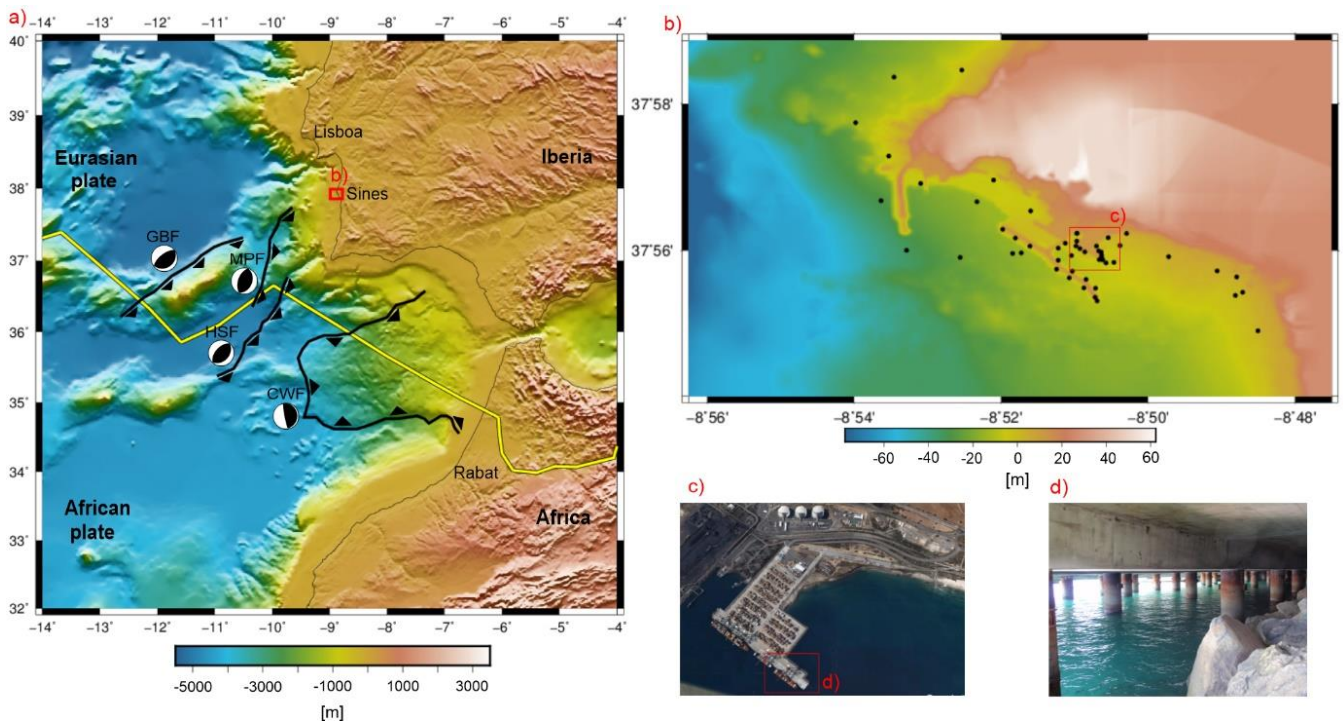


Fig. 1. Tsunami and earthquake action: a) seismic sources with tsunamigenic potential to affect Sines region (solid black lines and respective mechanisms characterized by the beach balls), and Eurasian and African tectonic plates divided by solid yellow line; b) high-resolution topo-bathymetry of the Sines region and localization of the virtual sensors considered in the numerical simulation; c) aerial view of the containers terminal, a pile supported quay, and d) a photography of the pile-supported quay structure (adapted from Reis, 2019 [31]).

The Sines port is an open deep-water seaport, with more than 2000 *ha*. Terminal XXI is a 1150 *m* long and more than -17m *zH* natural depth container terminal, handling a 2100000 *TEU* capacity. The Terminal XXI, Fig. 1c and 1d, is expanding to an additional 216 *m* longitudinal x 36.3 *m* transversal platform with five longitudinal bays, directly supported by piles transmitting the loads to the soil.

The average 25.5 *m* long piles have circular section of 1.3 *m* diameter and are embedded in a two-layered soil profile. The first layer is the triangular back landfill, the second layer is the bedrock foundation, in which the piles are 4 *m* embedded.

The superstructure is composed of longitudinal and transversal beams (see Fig. 2). The longitudinal beams are constructed with pre-cast pre-stressed formwork elements supporting cast-in-place RC beams. In alignment A and B, the beams cross-section is 8.00 *m* x 2.00 *m*, alignments C, D and E is 1.65 *m* x 1.65 *m* sections. In the longitudinal direction, the piles are 6 *m* spaced in Alignment A and E, while in B, C and D are 12 *m*. The transversal beams have cross-section 1.50 *m* x 1.00 *m* (quay 1) and the quay deck is a 0.25 *m* pre-cast slab supporting 0.20 *m* of cast-in-place RC flat slab (quay 2) [32]. Fig. 2 depict the general plant and typical transversal section adopted to for the FEM model.

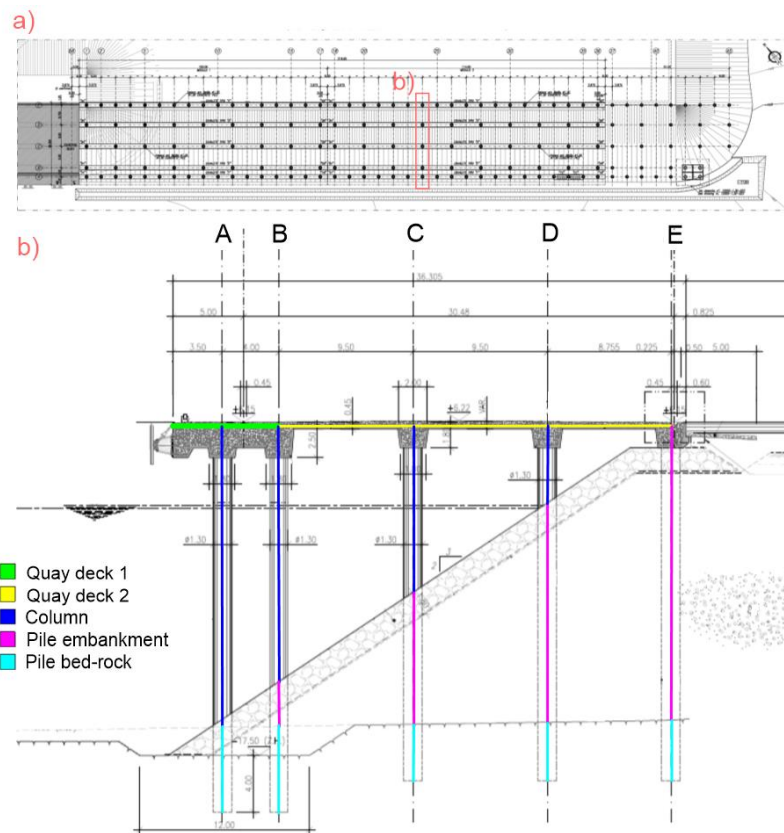


Fig. 2. Structural model: a) general plant of the existent and new pile-supported expansion of Terminal XXI - container terminal; b) transversal section of the pile-supported quay used to model the structure, and representation of the structural elements of the 2D model of the structure.

3.1 Tsunami and earthquake actions

To quantify the tsunami and earthquake actions, we performed a deterministic multi-targeted-hazard assessment considering different scenarios, oriented to the Sines port structure (for detailed description of the hazard assessment in Terminal XXI, see Reis, 2019 [31]).

Due to the structural design, we assume the tsunami as the constraining action to define both the tsunami and the ground motion design actions, meaning that the source that triggered the tsunami worst-case scenario for the structure is adopted to define the corresponding ground motion acceleration, contributing for a coherent succession of loadings and to avoid an over-conservative design.

The initial task is the selection of the sources used to establish the scenarios, following previous deterministic and probabilistic investigations of tsunami hazard in the Northeast Atlantic coasts [20] [21]. These studies demonstrate the tsunamigenic nature of the SWIM zone, including the potential to trigger a 1755-like event. Additionally, these studies provide reference information on the most-damaging scenarios and data to validate our simulations. By comparing our numerical solution with bibliographic data at some locations, we increase the reliability of our measures along the propagation path and in the vicinity of the port structure.

The probable scenarios are defined by selecting four typical faults of the northeast-southwest striking thrust system of the SWIM zone, shown in Fig. 1a: the Goringe Bank fault, GBF, Horseshoe fault, HSF, Marques de Pombal fault, MPF, and the composite failure of HSF and MPF, HSMPF. Using their location,



geometry and displacement, we compute the respective tsunami initial deformations, based on the Okada's theory implemented in Mirone suite [26]. For the tsunami simulation, we use high-resolution topo-bathymetric data [21]. The computation is performed by a well-balanced finite volume code that solves the Shallow Water equations, Kotkot [22] [23]. The simulation provides inundation depth and flow velocity measured at fifty virtual points, depicted in Fig. 1b. The implementation of the points in the Sines region, aim to compare our solution with solutions from previous studies (in terms of wave amplitude and tsunami travel time), and, the ones around the port and the quay, aiming to determine the worst-case scenario and the part of the quay structure more exposed to the tsunami action.

The obtained solutions verify the maximum amplitudes and tsunami travel time simulated by other authors, for the Sines region. The faults that triggered the tsunami worst case scenario were HSF and HSMPF. Nevertheless, the most damaging scenario (inundation depth and velocity) to Terminal XXI itself was assessed. This assessment allows to conclude that the tsunami worst case scenario for the structure is not coincident to the worst case scenario of the region, showing the importance of the wave(s) directivity, and leading to the selection of the GBF as the tsunami worst-case scenario for the pile-supported quay structure. Was also assessed the part of the structure more exposed to the tsunami. By comparing the virtual sensors implemented around the structure, the one implemented at the southeast extremity of the structure recorded the peak velocity (8,7 m/s) and inundation depth (15 m), implying that the higher solicitation of occurs at this point.

Using the time histories of both hydrodynamic quantities, wave height h and velocity u , we estimated the tsunami hydrodynamic action as recommended by ASCE design code [3]. Was assumed $\rho = 1.2 \text{ kg/m}^3$, $C_d = 2$, $C_{cx} = 0.5$, $C_u = 3$, $I_{tsu} = 1.25$. The hydrodynamic force in the in the horizontal direction follows Eq (2), and the maximum force is quantified as 1220 kN/m, while, following Eq (3), the hydrodynamic force in vertical direction is quantified as 5000 kN/m. A brief comment on the assessment of the tsunami forces: the FVM is used to compute free-surfaces, hence, the hydrodynamic quantities were assessed at the boundary between the fluid and the structure, leading to uncertainties of fluid behavior under the significative area of the quay. An immediate phenomenon, requiring a complementary fluid-structure-interaction model, is the conversion of horizontal into vertical hydrodynamic forces due to the triangular geometry of the backfill.

For the correspondent seismic action of the GBF scenario, we generated ten accelerograms to be imposed at the foundation of the structure. The peak ground motion acceleration, around 150 cm/s² (or 0.153 g), is coherent with the Eurocode 8 Portuguese National Annex, ranging between 125 – 150 cm/s², for rock and soft soils in Sines [15].

3.2 Structural model

The soil-structure system is modelled using a 2D model developed in OpenSees framework [30]. The typical transversal section and respective schematic FEM model is schematically represented in Fig. 2b. The RC structure consists of a quay deck supported by five circular RC columns/piles with 1.3 m of diameter, responsible for the direct transmission of the loads to the soil. The frame is modeled as RC beams and columns with non-linear distributed plasticity, using *Force-based Beam-Column* elements with *Force-Deformation* fiber sections, defined in terms of geometry and material. The geometry of the cross sections considers confined concrete, a cover of 6 cm as unconfined concrete and reinforcement steel bars. The concrete and steel materials respectively follow *Concrete04* and *Steel02* materials. To the *Concrete04* material, confined and unconfined sections, is assigned the strength class C35/45. To the *Steel02* material is assigned the steel grade A500. The model is discretized into structured quadrilateral elements with 0.5 m, to keep the numbers of elements low, reducing the computational time; and 1.5 weight at the line ends, to obtain better results near to the members edges, where plasticity is typically concentrated.

3.2 Structural analysis and discussion

The first interval of the analysis regards the static analysis due to the gravity loads. It contains boundary conditions, masses and gravity loads (dead and live loads). The *Static* with *Load-Control* integrator interval



solves the *BandGeneral* system of equations using a *Full Newton-Raphson* algorithm. The dead load is automatically computed from the cross-sectional properties and the specific weight of the frame elements geometry. *Linear-type* gravity loads are applied in 10 steps and are maintained until the end of the analysis, so Interval 2, regarding the seismic action, continues from the end of the gravity analysis. The tolerance of the *Norm Displacement Increment* convergence criteria is set to 10^{-8} allowing 100 interactions/step. A modal analysis was performed to characterize the modal periods and the Rayleigh damping. The period of the first mode is $T = 1.292$ s while the second mode $T = 0.89$ s. Damping ratio was considered $\xi = 0.05$.

The second interval regards the non-linear dynamic analysis, considering the ten different signals generated with GBF source parameters. The ground motion is imposed at the bed-rock level. At this stage, and for the sake of simplicity of the model, we didn't consider the backfill. The implications of this assumption are, on one hand, it would be an additional mass for the seismic excitation, on the other hand, it is a tradeoff between the decreasing of horizontal displacements, and the shortening on the pile length, increasing the deformation. The *Transient* analysis uses *Newmark* integration scheme. The convergence is tested with *Norm Displacement Increment* with tolerance of to 10^{-5} , 100 interactions/step. To satisfy the dynamic equilibrium at discrete time-steps, mainly due to non-linear behavior of the structure, the stiffness of the system may require iterations due to degradation of strength and redistribution of forces. The duration of the analysis is set to 60 s, to cover up the stages from rest to excited to rest stages. The load, *Uniform Excitation* type in U_x direction (horizontal excitation), is given by a *Record* file and is maintained until the end of the analysis, so the Interval 3 continues from the end of this analysis.

From the seismic analysis, we assessed the range of response displacements of the structure, in Fig. 3c. The horizontal displacement of the structure is maximum at the interaction between the piles and the quay, varying from $\delta_x = 5.9$ cm to 12 cm, being the average maximum horizontal displacement, considering all the excitation signals, $\delta_{x,max\ average} = 6.2$ cm.

The range of structural response values, for the different signals, are: 1) for the deformations: $\theta_{str} = 0.10^\circ$ to 0.16° , and 2) for forces: $M_{sd} = 1950$ kNm to 4850 kNm. When compared with the capacity of the pile, bottom and top sections (Fig. 3a), is observed that 20% of the accelerograms lead to the development of plastic hinges, most likely to be formed at the top of the piles in alignments D and E (identified in Fig. 2b). Nevertheless, as a recent structure, following the Eurocode performance-design recommendations, the structure was designed to guarantee the significant damage criteria (non-collapse, but important deformations are allowed). The European EC8 has reference values for buildings and the American PIANC recommends values for ports [33]. All the obtained values of maximum rotation respect the European EC8 relation $\theta_{str} < 6 \theta_{yielding}$, and the American PIANC $\theta_{str} < 3^\circ$ recommendation. The range of values herein presented are coherent with the magnitude of values used to design the quay [32]. In Fig. 3a and b are depicted the capacity curve of the pile and one of the determined moment-rotation diagrams, computed at the top of pile from alignment E. In the depicted moment-rotation diagram, which is the structural response to acceleration 8, the structure remained in elastic regime. This is the equivalent to a far-field tsunami situation.

Finally, Interval 3 regards the non-linear dynamic analysis of the tsunami, considering the horizontal hydrodynamic effect combined with a boundary condition from the seismic analysis. The transient non-linear analysis used *Newmark* scheme of integration, being the convergence assessed by *Norm Displacement Increment* with 10^{-5} tolerance, 500 interactions/step. For the sake of representativity, we adopted the solutions of accelerogram 1, elasto-plastic regime, and accelerogram 8, elastic regime, resembling a near- and a far-field tsunami, respectively. The dynamic lateral force of the tsunami is applied as a pattern of a nodal forces, defined by a *Function*, applied along the height of the structure. As expected, the moment-rotation diagram of both cases are overcovered: 1) the accelerograms are generated by the same source parameters, resulting in slightly differences, and 2) the classification of the structure as elastic or elasto-plastic regime structure differ merely 500 kNm in the plastic hinge formed at the top of piles E and D. Fig. 3d depicts the moment-rotation diagram.

The magnitude of solicitations-structural response values, in Interval 2 (Fig. 3b) and Interval 3 (Fig. 3d), is remarkable and demonstrates the importance to consider the tsunami as a design load. The average structural



solicitations due to the ground motion are about $M_{sd} = 3000 \text{ kNm}$, below the yielding level, while in the combination of earthquake and tsunami, $M_{sd} = 7000 \text{ kNm}$. Respectively, the average deformations are $\theta_{str} = 0.14^\circ$ and $\theta_{str} = 0.20^\circ$.

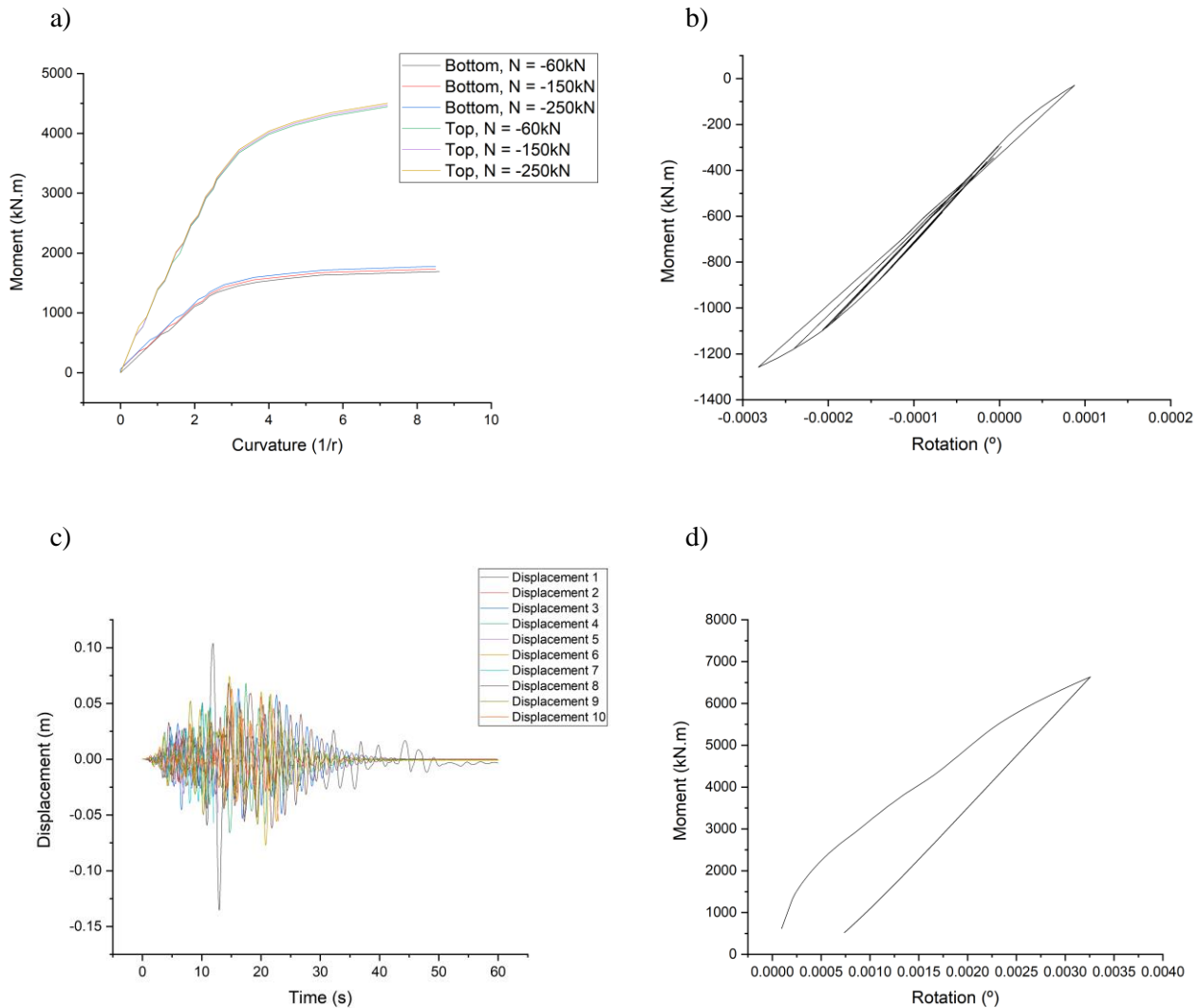


Fig. 3. Structural analysis: a) structural capacity of the piles, b) diagram moment-rotation of the pile submitted to the ground motion, c) structural response to the accelerogram in terms of horizontal displacements; d) diagram of moment-rotation of the pile submitted to cascading earthquake and tsunami.

Due to the vertical component of the tsunami, the first approach, by comparing gravity and vertical hydrodynamic loads, directly demonstrates the importance to adopt design measures against the tsunami effects, i.e.: 1) the structure is not designed for ascending forces; 2) the uplifting/vertical hydrodynamic effect is greater than the combination of dead and live loads, mass of water above the quay and debris transportation, if overtopping occurs.

4. Conclusions

Considering the tsunamigenic sources from the SWIM area, HSF and HSMPF triggered more hazardous tsunamis for the Sines region, however, due to its directivity, the GBF constitutes the tsunami worst-case scenario, with wave heights up to $h = 15 \text{ m}$ and velocity up to $u = 8,8 \text{ m/s}$.



Commonly, design codes are oriented to the seismic action, estimated for the Sines region as $0.153 g$. The case study herein described highlights the importance to have additional measures to mitigate the effects of a tsunami. The value of the average structural solicitation due to the ground motion is less than half the solicitations considering the combined actions, whose rotational deformation doubles the rotation provoked by the ground motion. In open-type wharves, a differentiating factor is the occurrence of tsunami overtopping, hence that the vertical hydrodynamic force is more damaging than the horizontal, and the pile-supported quays are exclusively designed to resist descending solicitations, leading to the uplifting of the system quay-piles.

5. Future work

The ASCE design code suggest analytic and/or numeric approaches to quantify the tsunami force exerted against a structure, function of the structure importance. We will use a complementary Smoothed Particle Hydrodynamic, SPH, method to perform a purely numerical assessment of the tsunami force exerted against the structure. To optimize the elevated computational demand associated to SPH, we will couple our Eulerian FVM to the meshless Lagrangian SPH. Another contribution of the SPH is the more accurate assessment of the vertical hydrodynamic force, hence that FVM is not appropriate to simulate this level of complexity regarding the free surface.

Due to the structural model, will be included the ships mooring, and moving loads associated with cranes and reach stackers when defining the live load. The influence of the dimensions of the model, 2D vs. 3D will be assessed. The goal is to characterize the conversion of a 3D physical problem into a 2D model, where the tsunami lateral force, even affected by a closure coefficient, interprets the quay as a closed-type instead of an open-type wharf. The application of the tsunami in the will also be investigated. The influence of the soil and the level of representations of structure-foundation-soil systems, discrete vs. continuum, will also be considered in the parametric study of the structural modeling and analysis.

In the 2011, Tohoku event, a team of experts surveyed structures along 600 km of the coast. They highlighted the important role played by the structures of coastal defense played in the mitigation of more severe damage in the coastal structures. We will assess the influence of their presence, location of implementation and orientation, considering a range of synthetic tsunami scenarios.

6. Acknowledgements

The first author is supported by Fundação para a Ciência e Tecnologia, PhD grant no. SFRH/BD/137531/2018, ongoing at Lisbon University, Instituto Superior Técnico, Civil Engineering Research and Innovation for Sustainability (CERIS). The authors acknowledge the financial support provided by: the Fundo Europeu de Desenvolvimento Regional, through the Programa Operacional Fatores de Competitividade and the National Funds through the Fundação para a Ciência e Tecnologia, project no. POCI-01-0145-FEDER-028118; the scholarship awarded by the Administração dos Portos de Sines e do Algarve, S.A.; the scholarship awarded by CERIS. The authors acknowledge the data from: the Sines high-resolution topo-bathymetry provided by work developed in the framework of the ASTARTE international project; the generation of the seismic accelerograms provided by Dra Alexandra Carvalho, from Laboratório Nacional de Engenharia Civil; and, at least, the structural design provided by the Administração dos Portos de Sines e do Algarve, S.A..

7. References

- [1] F. Imamura, S. Boret, A. Suppasri and A. Muhari, "Recent occurrences of serious tsunami damage and the future challenges of tsunami disaster risk reduction," *Progress in Disaster Science*, vol. 1, no. 100009, 2019.
- [2] United Nations, "Sendai Framework for Disaster Risk Reduction 2015-2030," United Nations Office for Disaster Risk Reduction at the, 3rd UN World Conference, Sendai, Japan, 2015.



- [3] A. S. o. C. E. ASCE, "Chapter 6 - Tsunami Loads and Effects," in *Standard, Minimum Design Loads and Associated Criteria for Buildings and Other Structures*, 2016.
- [4] I. T. a. T. Ministry of Land, "Further Information Concerning the Design Method of Safe Buildings that are Structurally Resistant to Tsunamis - Technical Advice No. 2570," MLIT, Tokyo, Japan, 2011.
- [5] M. Alam, A. Barbosa, M. Scott, D. Cox and J. van de Lindt, "Multi-hazard earthquake-tsunami structural fragility assessment framework," in *13th International Conference on Applications of Statistics and Probability in Civil Engineering, ICASP13*, Seoul. South Korea, 2019.
- [6] D. Chakraborty and D. Choudhury, "Stability of Non-Vertical Waterfront Retaining Wall Supporting Inclined Backfill under earthquake and tsunami," *Ocean Engineering*, vol. 78, pp. 1-10, 2014.
- [7] k. Lee, D. Kim and T. Kim, "Extreme Case Study of Quay Wall Stability Under Earthquake and Tsunami," *Marine Georesources and Geotechnology*, vol. 33, no. 6, pp. 504-520, 2015.
- [8] T. Rossetto, C. Petrone, I. Eames, C. Barra, A. Foster and J. Macabuag, "Chapter 23 - Advances in the Assessment of Buildings Subjected to Earthquakes and Tsunami," in *Geotechnical, Geological and Earthquake Engineering*, Springer International Publishing AG, 2018, pp. 545-562.
- [9] T. Carey, H. B. Mason, A. Barbosa and M. Scott, "Multihazard Earthquake and Tsunami Effects on Soil–Foundation–Bridge Systems," *Journal of Bridge Engineering*, vol. 24, no. 4, 2019.
- [10] I. Charvet, J. Macabuag and T. Rossetto, "Estimating tsunami-induced building damage through fragility functions: Critical review and research needs," *Frontiers in Built Environment - Earthquake engineering*, vol. 3, p. 36, 2017.
- [11] T. Sugano, A. Nozu, E. Kohama, K. Shimosako and Y. Kikuchi, "Damage to coastal structures," vol. 54, no. 4, pp. 883-901, 2014.
- [12] S. P. Vilanova and J. F. Fonseca, "Probabilistic seismic-hazard assessment for Portugal," *Bulletin of the Seismological Society of America*, vol. 97, no. 5, pp. 1702-1717, 2007 .
- [13] J. Zizmond and M. Dolsek, "Risk-targeted force-based design and performance check by means of nonlinear analysis," in *Tenth Pacific Conference on Earthquake Engineering Building and Earthquake-Resiliency*, Sydney, Australia, 2015.
- [14] N. Luco, B. Garret and J. Hayes, "New Risk-Targeted Seismic Maps Introduced into Building Codes," National Earthquake Hazard Reduction Program, 2012.
- [15] Brussels: European Committee for Standardization , Eurocode 8: Design of Structures For Earthquake Resistance - Part 1: General Rules, Seismic Actions and Rules for Buildings, Brussels, 2005.
- [16] V. Silva, H. Crowley and P. Bazzurro, "Exploring risk-targeted hazard maps for Europe," *Earthquake Spectra*, vol. 32, no. 2, 2015.
- [17] J. Douglas and A. Gkimprxis, "Using targeted risk in seismic design codes: a summary of the state of the art and outstanding issues," in *6th National Conference on Earthquake Engineering and 2nd National Conference on Earthquake Engineering and Seismology*, Bucharest, Romania, 2017.
- [18] A. Raby, J. Macabuag, A. Pomonis and S. Wilkinson, "Implication of the 2011 Great East Japan tsunami on sea defence design," *International Journal of Disaster Risk Reduction*, vol. 14, pp. 332-346, 2015.
- [19] J. C. Duarte , F. M. Rosas, P. Terrinha, W. P. Schellart , D. Boutelier, M. A. Gutscher and A. Ribeiro, "Are subduction zones invading the Atlantic? Evidence from the Southwest Iberia Margin," *Geology*, vol. 41, no. 8, pp. 839-842, 2013.



- [20] R. Omira, M. A. Baptista and L. Matias, "Probabilistic tsunami hazard in the Northeast Atlantic from near- and far-field tectonic sources," *Pure and Applied Geophysics*, vol. 172, no. 3-4, pp. 901-920, 2014.
- [21] M. Wronna, R. Omira and M. A. Baptista, "Deterministic approach for multiple-source tsunami hazard assessment for Sines, Portugal," *Natural Hazards and Earth System Sciences*, vol. 15, pp. 2557-2568, 2015.
- [22] S. Clain, C. Reis, R. Costa, J. Figueiredo, M. A. Baptista and J. M. Miranda, "Clain, S., Reis, C., Costa, R., Figueiredo, J., Baptista, M. A., & Miranda, J. M. (2016). Second-order finite volume with hydrostatic reconstruction for tsunami simulation," *Journal of Advances in Modeling Earth Systems*, 8(4), 1691-1713., vol. 8, no. 4, pp. 1691-1713, 2016.
- [23] C. Reis, J. Figueiredo, S. Clain, R. Omira, M. A. Baptista and J. M. Miranda, "Comparison between MUSCL and MOOD techniques in a finite volume well-balanced code to solve SWE. The Tohoku-Oki, 2011 example," *Geophysical Journal International*, vol. 216, no. 2, pp. 958-983, 2018.
- [24] N. Sharma, K. Dasgupta and A. Dey, "Optimum lateral extent of soil domain for dynamic SSI analysis of RC framed buildings on pile foundations," *Frontiers of Structural and Civil Engineering*, pp. 1-20, 2019.
- [25] Y. Okada, "Surface deformation due to shear and tensile faults in a half-space," *Bulletin of the seismological Society of America*, vol. 75, no. 4, pp. 1135-1154, 1985.
- [26] J. Luis, "Mirone: a multi-purpose tool for exploring grid data.," *Cumputer and Geosciences*, vol. 33, no. 1, pp. 31-41, 2007.
- [27] I. Beresnev and G. Atkinson, "FINSIM - A FORTRAN Program for Simulating Stochastic Acceleration Time Histories from Finite Faults," *Seismological Research Letters*, vol. 69, no. 1, pp. 27-32, 1998.
- [28] A. Carvalho, "Modelação estocástica da acção sísmica em Portugal continental," PhD thesis, Instituto Superior Técnico, Lisbon, Portugal, 2077.
- [29] D. Boore, "Stochastic simulation of high-frequency ground motions based on seismological models of the radiated spectra," *Bulletin of the Seismological Society of America*, vol. 73, no. 6A, pp. 1865-1894, 1983.
- [30] F. McKenna, "OpenSees: A Framework for Earthquake Engineering Simulation," *Computing in Science and Engineering*, vol. 13, no. 4, pp. 58-66, 2011.
- [31] C. Reis, "Pile-supported quay submitted to successive earthquake and tsunami actions," in *15th Triennial International Conference of Ports, PIANC, ASCE*, Pittsburg, Pennsylvania, 2019.
- [32] Administração dos Portos de Sines e do Algarve S.A, *Personal communication.*, 2017.
- [33] A. A. Balkema, *Seismic Design Guidelines for Port Structures.*, Rotterdam: PIANC, 2011.
- [34] M. A. Baptista, J. M. Miranda, R. Omira and C. Antunes, "Potential inundation of Lisbon downtown by a 1755-like tsunami," *Natural Hazards and Earth System Science*, vol. 11, no. 12, pp. 3319-3326, 2011.
- [35] A. Barbosa, H. B. Mason and K. Romney, "Soil-Bridge Interaction During Long-Duration Earthquake Motions," School of Civil and Construction Engineering, Oregon State University, Corvallis, Oregon, 2014.
- [36] M. Zhu, I. Elkhetafi and M. Scott, "Validation of OpenSees for Tsunami Loading on Bridges Superstructures," *Journal of Bridge Engineering*, vol. 23, no. 4, pp. 1-10, 2018.
- [37] G. Kang, D. Kim and T. Kim, "Quay Wall Stability Considering Earthquake and Tsunami Overtopping Forces Together in the Active Condition," *Natural Hazards Review*, vol. 15, no. 4, 2014.
- [38] B. Chaudhary, H. Hazarika, I. Ishibashi and A. Amizatulhani, "Sliding and Overturning Stability of Breakwater Under Combined Effect of Earthquake and Tsunami," *Ocean Engineering*, vol. 136, pp. 106-116, 2017.